

# SOPHIE velocimetry of *Kepler* transit candidates <sup>★,★★</sup>

## VI. A false positive rate of 35% for *Kepler* close-in giant candidates

A. Santerne<sup>1,3</sup>, R. F. Díaz<sup>1,2,3</sup>, C. Moutou<sup>1</sup>, F. Bouchy<sup>2,3</sup>, G. Hébrard<sup>2,3</sup>, J.-M. Almenara<sup>1</sup>, A. S. Bonomo<sup>1</sup>, M. Deleuil<sup>1</sup>,  
and N. C. Santos<sup>4,5</sup>

<sup>1</sup> Laboratoire d'Astrophysique de Marseille, Université d'Aix-Marseille & CNRS, 38 rue Frédéric Joliot-Curie, 13388 Marseille cedex 13, France

<sup>2</sup> Institut d'Astrophysique de Paris, UMR7095 CNRS, Université Pierre & Marie Curie, 98bis boulevard Arago, 75014 Paris, France

<sup>3</sup> Observatoire de Haute-Provence, Université d'Aix-Marseille & CNRS, 04870 Saint Michel l'Observatoire, France

<sup>4</sup> Centro de Astrofísica, Universidade do Porto, Rua das Estrelas, 4150-762 Porto, Portugal

<sup>5</sup> Departamento de Física e Astronomia, Faculdade de Ciências, Universidade do Porto, Portugal

Received: 2012/05/15 ; Accepted: ????

### ABSTRACT

The false positive probability (FPP) of *Kepler* transiting candidates is a key value for statistical studies of candidate properties. An investigation of the stellar population in the *Kepler* field by Morton & Johnson (2011) has provided an estimation for the FPP of less than 5% for most of the candidates. We report here the results of our radial velocity observations on a sample of 46 *Kepler* candidates with transit depth greater than 0.4%, orbital period less than 25 days and host star brighter than *Kepler* magnitude 14.7. We used the SOPHIE spectrograph mounted on the 1.93-m telescope at the Observatoire de Haute-Provence to establish the nature of the transiting candidates. In this sample, we found 5 undiluted eclipsing binaries, 2 brown dwarfs, 6 diluted eclipsing binaries and 9 new transiting planets that complete the 11 already published. The remaining 13 candidates were not followed up or remain unsolved due to photon noise limitation or lack of observations. From these results we compute the FPP for *Kepler* close-in giant candidates to be  $34.8\% \pm 6.5\%$ . We investigate the variation of FPP for giant candidates with the longer orbital periods and find that it should be up to 40% for orbital periods in-between 10 days and 200 days. We thus find a significant discrepancy with the estimation of Morton & Johnson (2011). We finally discuss the reasons of this discrepancy and the possible extension of this work towards smaller planet candidates.

**Key words.** planetary systems – techniques: photometric – techniques: radial velocities – techniques: spectroscopic

### 1. Introduction

Since 2009, the *Kepler* space mission (Borucki et al. 2010) is monitoring more than 150,000 stars with high precision photometry to search for transiting earth-like planets in the habitable zone. The unprecedented photometric precision reached by *Kepler* has permitted the discovery of the first validated transiting planet in the habitable zone (Borucki et al. 2012) out of the solar system as well as extrasolar planets with radius down to the size of the Earth (Fressin et al. 2012; Muirhead et al. 2012). The large number of planet candidates discovered so far (2321, Batalha et al. 2012, hereafter Ba12) was used to estimate the occurrence of planets around Solar-type stars (e.g. Howard et al. 2011, from the list of 1235 KOIs), in relative agreement with Doppler surveys (Howard et al. 2010; Mayor et al. 2011). However, this statistical analysis assumes that most planet candidates are real planets or at least, that the impostor rate is negligible. The experience gained in ground-based surveys or the pioneer space mission *CoRoT* (Baglin et al. 2006) show

that such false positives are mainly due to undiluted eclipsing binaries with a low-mass stellar companion (Moutou et al. 2008; Almenara et al. 2009) or diluted eclipsing binaries (so-called “blends”) whose eclipse depth is diluted with the target flux and can therefore mimic a planetary transit (e.g. Tal-Or et al. 2011). Statistical analysis of stellar populations in the Milky Way can provide estimations of the false positive rate (Brown 2003). A statistical study of the false positive probability (hereafter FPP) of the *Kepler* candidates has been performed by Morton & Johnson (2011) (hereafter M&J11). They find an overall FPP of less than 10% for 90% of the *Kepler* candidates with a median value close to 5%.

To establish the planetary nature of a transiting candidate, one must measure its mass through radial velocity (RV) follow-up (Bouchy et al. 2009b) or using the transit time variation technique (Holman et al. 2010). Another solution is to “validate” the candidate by excluding all false positive scenarios with a significant confidence level (the so-called “BLENDER” technique, e.g. Torres et al. 2011; Fressin et al. 2011). Establishing or validating the nature of planetary candidates for a significant sample of *Kepler* candidates can improve the true fraction of *Kepler* false positives and thus can improve the interpretation of *Kepler* planet population.

Send offprint requests to: Alexandre Santerne  
e-mail: alexandre.santerne@oamp.fr

<sup>\*</sup> Based on observations made with SOPHIE on the 1.93-m telescope at Observatoire de Haute-Provence (CNRS), France

<sup>\*\*</sup> RV data is only available at the CDS via anonymous ftp to cdsarc.u-strasbg.fr (130.79.128.5) or via http://cdsarc.u-strasbg.fr/viz-bin/qcat?J/A+A/vol/page

In this paper, we first-of-all present our selection of *Kepler* giant planet candidates (section 2) and their nature (section 3). We establish the candidate's nature using the SOPHIE spectrograph at Observatoire de Haute-Provence. Our results allow us to independently measure the *Kepler* FPP of such giant candidates (section 5) and to compare it with other estimations (6.1, 6.2). We finally estimate the trend of false positive rate for longer period giant planets (section 6.3) and the impact of this new FPP value on the exoplanet statistics (section 6.4).

## 2. Selection of *Kepler* candidates

Initially, a first list of 306 *Kepler* planetary candidates was published in June 2010 by [Borucki et al. \(2011a\)](#). This list contained only the candidates transiting stars with *Kepler* magnitude  $K_p > 14$ . Out of this list, our team selected four candidates to follow-up with the SOPHIE spectrograph during the summer 2010 ([Bouchy et al. 2011](#)). These observations led to the discovery of the two first planets established from the public data: KOI-428b ([Santerne et al. 2011b](#)) and KOI-423b ([Bouchy et al. 2011](#)). In February 2011, the public list of candidates was extended up to 1235 candidates ([Borucki et al. 2011b](#)), and to 2321 candidates in February 2012 (Ba12) including the brighter targets.

From the [Borucki et al. \(2011b\)](#) list and then from the Ba12 list of Kepler Objects of Interest (KOI), we defined a sample of candidates to follow-up with the SOPHIE spectrograph: we first removed all the targets with  $K_p > 14.7$  which corresponds to the magnitude limit of the SOPHIE spectrograph ([Santerne et al. 2011a](#)). About 49% of *Kepler* candidates are orbiting around such faint stars. We then rejected all the candidates whose transit depth is shallower than 0.4% in flux. We preferred selecting targets based on their transit depth rather than their expected radius because candidate radii are derived using the estimation of the stellar radius that could have up to 30% of uncertainty ([Borucki et al. 2011b](#)). We decided first of all to focus on short-orbital period giant planet candidates and kept only the candidates with orbital period shorter than 25 days. Indeed, all the known transiting planets with a transit deeper than 0.4% and orbital period less than 25-day have a radial velocity semi-amplitude greater than  $10 \text{ m s}^{-1}$ . This limit is close to the photon noise reached by SOPHIE in 1-h exposure time on a  $\sim 13^{\text{th}}$  magnitude star. Out of the 2321 KOIs, only  $\sim 3.8\%$  present both a star brighter than  $K_p = 14.7$  and a transit depth greater than 0.4%. If we keep only the shortest orbital period ( $P < 25$  days),  $\sim 2.3\%$  candidates remained. Finally, we removed the 8 candidates with a vetting flag<sup>1</sup> of 4 in [Borucki et al. \(2011b\)](#) that match all the previous criteria. Indeed, out of these 8 lowest priority candidates, most of them are either clear eclipsing binaries with transit depths up to 8% or show in their light curve a high level of variability due to a high rotating or pulsating host star.

Only 46 candidates respect all the criteria which correspond to about 2% of the total list of the 2321 candidates as of February 2012 and to about 22% of all the giant planet candidates (with depth  $> 0.4\%$ ) found by *Kepler* up to now. About 60% of the *Kepler* giant planet candidates are orbiting stars fainter than  $K_p = 14.7$ . The 46 selected candidates, with their parameters, are listed in Table 1. We note that only 2 candidates in this

sample are in a multiple system: KOI-94.01 and KOI-377.01 (*Kepler*-9b). We also note that only 2 candidates were added with the updated list of KOIs from Ba12: KOI-554.01 and KOI-1786.01.

## 3. SOPHIE observations

### 3.1. Observations and data reduction

We started a new large program in early 2011 to perform spectroscopic follow-up observations on the 46 selected *Kepler* targets with the SOPHIE spectrograph ([Perruchot et al. 2008](#); [Bouchy et al. 2009c](#)) mounted on the 1.93-m telescope at Observatoire de Haute-Provence, France. Observations were conducted from 2011, February 24 to 2012, May 2 using the High Efficiency mode ( $R \sim 39\,000$  at 550nm) of SOPHIE<sup>2</sup>. Spectra were reduced with the online standard pipeline and radial velocities were obtained by computing the weighted cross-correlation function (CCF) of the spectra with a numerical spectral mask of a G2V star ([Baranne et al. 1996](#); [Pepe et al. 2002](#)). For some candidates, we also correlate the CCF using a F0V and K5V mask in order to test the mask effect ([Bouchy et al. 2009b](#)).

Several spectra were significantly affected by the scattered moon light and corrected using the same technique as in [Santerne et al. \(2011b\)](#) and [Bonomo et al. \(2010\)](#). We tried to keep the signal-to-noise ratio (S/N) as constant as possible to limit the charge transfert inefficiency effect of the CCD camera ([Bouchy et al. 2009a](#)). We corrected the radial velocities of a given target that were computed from different S/N spectra with the equation 1. This empirical function was calibrated with dedicated observations with SOPHIE at different S/N spectra of the daily blue sky:

$$\Delta RV(\text{SNR}_{550\text{nm}}) = -6.265 \times (\text{SNR}_{550\text{nm}})^{-1.71} [\text{m s}^{-1}] \quad (1)$$

where  $\text{SNR}_{550\text{nm}}$  is the signal-to-noise ratio per pixel measured on the extracted spectrum in the range 10 – 50. We also computed the  $v \sin i_*$  using Appendix B.1. in [Boisse et al. \(2010\)](#). The radial velocities are listed in Tables 2 to 16.

### 3.2. Spectroscopic analysis

For the candidates that do present a significant radial velocity variation, we performed a detailed spectroscopic analysis to determine their stellar parameters in order to derive the candidate parameters. For the low-rotating ones (namely KOI-192, KOI-197 and KOI-201) this analysis was based on iron line excitation and ionization equilibrium. This analysis made use of a grid of [Kurucz \(1997\)](#) model atmospheres and of the 2002 version of the radiative transfer code MOOG ([Sneden 1973](#)). For details we point the reader to [Santos et al. \(2004\)](#) and [Sousa et al. \(2008\)](#).

The spectroscopic analysis is based on the measurement of line equivalent widths (EWs) for a list of selected Fe I and Fe II lines. For this we used the stacked SOPHIE spectra used for the derivation of radial velocities. For KOI-197, the spectrum had a total S/N high enough (around 50 at 6700Å) so that we made use of the automatic code ARES ([Sousa et](#)

<sup>1</sup> According to [Borucki et al. \(2011b\)](#), a vetting flag of 4 means : “Insufficient follow-up to perform full suite of vetting tests”.

<sup>2</sup> prog. IDs: 11A.PNP.MOUT, 11B.PNP.MOUT, 12A.PNP.MOUT

al. 2007) to measure the EWs for the almost 300 lines used in the analysis. For KOI-192 and KOI-201, given the low S/N (around 20) of the available spectra we decided to adopt a more careful analysis. We then adopted the shorter (but well tested) line-list presented in Santos et al. (2004) and the EWs were carefully measured one by one using the *splot* tool of IRAF.

We finally determined the stellar mass, radius and age by comparing the  $\log g$ ,  $T_{\text{eff}}$ , and  $[\text{Fe}/\text{H}]$  from the stellar analysis to the STAREVOL evolution tracks (Turck-Chièze et al. 2010), in the ( $T_{\text{eff}}$ ,  $\log g$ ) H-R diagram.

For the fast-rotating no-variation candidates (namely KOI-12, KOI-131 and KOI-611), the resulting co-added spectrum S/N was too low to allow spectral analysis. We thus consider the stellar parameters from Ba12 in our analysis.

## 4. Establishing the nature of KOIs

In this section, we discuss the results obtained on individual candidates. Stellar masses and radii come from the *Kepler* Input Catalog (Brown et al. 2011), but the 3 aforementioned.

### 4.1. Secure planets

Our selection of 46 KOIs include three pre-launch planets: KOI-1.01, KOI-2.01 and KOI-3.01, also named, TrES-2 (O'Donovan et al. 2006), HAT-P-7b (Pál et al. 2008) and HAT-P-11b (Bakos et al. 2010), respectively. It also includes the four planets announced by the *Kepler* team in early 2010 : KOI-18.01 / Kepler-5b (Koch et al. 2010), KOI-17.01 / Kepler-6b (Dunham et al. 2010), KOI-97.01 / Kepler-7b (Latham et al. 2010) and KOI-10.01 / Kepler-8b (Jenkins et al. 2010). One planet of the KOI-377 / Kepler-9 system (Holman et al. 2010) is also present in our sample. In 2011, the *Kepler* team established the planetary nature of KOI-20.01 / Kepler-12b (Fortney et al. 2011), KOI-127.01 / Kepler-15b (Endl et al. 2011) and KOI-203.01 / Kepler-17b (Désert et al. 2011) that were also in our KOI selection. At the time of the publication of the latter one, eight SOPHIE spectra had been acquired that permit to independently confirm and improve the planet and stellar parameters (Bonomo et al. 2012).

Another planet from this list has also been characterized and announced: KOI-13.01 for which an upper-limit on the mass in the planet regime was performed using the photometric beaming effect (Shporer et al. 2011; Mazeh et al. 2011) and ellipsoidal effect (Mislis & Hodgkin 2012).

Finally, based on our observations obtained with the SOPHIE spectrograph, we found nine new planets in this sample: KOI-135b (Bonomo et al. 2012), KOI-196b (Santerne et al. 2011c), KOI-200b (Hébrard et al., in prep.), KOI-202b (Hébrard et al., in prep.), KOI-203b / Kepler-17b (Bonomo et al. 2012), KOI-204b (Bonomo et al. 2012), KOI-206b (Hébrard et al., in prep.), KOI-423b (Bouchy et al. 2011) and KOI-680b (Hébrard et al., in prep.). We also found KOI-428b (Santerne et al. 2011b). Since its transit depth is about 0.3% due to the large radius of the host star, this hot jupiter is not included in our sample.

For this study, we consider the upper mass limit of planet proposed by Schneider et al. (2011) of up to  $25M_{\text{Jup}}$ . Out of the 46 candidates we selected, 20 turned out to be planets

### 4.2. Brown Dwarfs

We found two interesting objects that have a mass in-between  $25M_{\text{Jup}}$  and  $80M_{\text{Jup}}$ . We classified these candidates as new transiting brown dwarfs but do not consider them as planet for the computation of the false positive rate. These objects are KOI-205.01 and KOI-554.01 that have a mass of about  $35M_{\text{Jup}}$  and  $80M_{\text{Jup}}$  respectively (Díaz et al., in prep.).

### 4.3. Undiluted binaries

By following-up the *Kepler* candidates, we found several targets that present large radial velocity variations which are not compatible with a planetary scenario. These candidates are thus undiluted eclipsing binaries:

#### KOI-340.01

KOI-340.01 is a candidate on a  $\sim 23.7$  day-period orbit with a depth of 2.12%. We observed this target twice with SOPHIE (see Table 8 and Fig. 1). We found a large radial velocity variation with a semi-amplitude of  $K = 34.577 \pm 0.074 \text{ km s}^{-1}$  assuming a circular orbit. If the stellar mass is  $1.15M_{\odot}$  (Ba12), the transiting companion would have a mass of  $0.70 \pm 0.04M_{\odot}$ , and thus be an eclipsing binary. No secondary peak is visible in the CCF nor clear secondary eclipse in the *Kepler* LC. We suspect that the host star is an evolved star that would also explain both the quite long-transit duration (14.4h) and a shallow eclipse for this eclipsing binary. We note that this planetary candidate is also classified as an eclipsing binary in the *Kepler* eclipsing binary catalog<sup>3</sup>. This candidate have been estimated by M&J11 to be a diluted binary (see discussion section 6.1) with a probability of 100% due to the very low likelihood of the planet scenario.

#### KOI-419.01

We visited KOI-419 seven times with SOPHIE. KOI-419.01 orbits its host-star in a  $\sim 20.1$ -day period. The radial velocities listed in Table 10 and displayed in Fig. 1 show a clear radial velocity variation in anti-phase with *Kepler* ephemeris. We analyzed both the *Kepler* PDC LC (Q1 to Q6) filtered using an iterative smoothing filter keeping the period of the signal, the SOPHIE RVs and the available SDSS, 2MASS (Skrutskie et al. 2006) and WISE magnitudes. We modeled a binary scenario using stellar atmosphere models of Castelli & Kurucz (2004), light-curve models from JKTEBOP (Southworth 2008) and evolution tracks from Marigo et al. (2008); Girardi et al. (2010). The model parameters were fitted through a MCMC simulation (Santerne et al., in prep.). We fixed the orbital period to the one published by Ba12 and fitted the eccentricity, the inclination, the argument of periastron, the systemic radial velocity. We assumed a binary system with two stars with the same  $\log(\text{age})$  and metallicity that we allow to vary and fitted both initial masses, system distance and reddening coefficient. We find that the data are compatible with an eccentric binary ( $e \sim 0.33$ ) for which only the secondary eclipse occurs (see fig 7). All the parameters derived from this combined analysis are provided in Table 17. We found a primary and secondary mass to be  $1.25 \pm 0.12 M_{\odot}$  and  $0.72 \pm 0.07 M_{\odot}$ , respectively. The system is thus an eclipsing binary.

<sup>3</sup> [http://archive.stsci.edu/kepler/eclipsing\\_binaries.html](http://archive.stsci.edu/kepler/eclipsing_binaries.html)



## KOI-607.01

KOI-607.01 is a  $\sim 5.9$  days period candidate. We took two SOPHIE measurements (see Table 12 and Fig. 1) that present radial velocity variations in phase with *Kepler* ephemeris. Assuming a circular orbit, we find  $K = 13.45 \pm 0.06 \text{ km s}^{-1}$ . If the mass of the host star is  $0.79 M_{\odot}$  (Ba12), the mass of the companion is  $0.106 \pm 0.006 M_{\odot}$ . This interesting low-mass star do not show a significant secondary eclipse at phase 0.5.

## KOI-698.01

We observed three times with SOPHIE the candidate host KOI-698. The transits occur every  $\sim 12.7$  days. The measured radial velocities (see Table 15 and Fig. 1) show a large variation in anti-phase with the *Kepler* ephemeris. As for KOI-419, we analyzed both the *Kepler* PDC LC (Q2 to Q6) using the same filtering method, the SOPHIE RVs and magnitudes from SDSS, 2MASS (Skrutskie et al. 2006) and WISE. We performed the same simulation using the same fixed and free parameters. As for KOI-419, we found that the system is also compatible with an eccentric binary ( $e \sim 0.4$ ) for which the primary transit is unseen (see fig. 8). All the parameters derived from this combined analysis are provided in Table 18 and lead to a primary and secondary mass of  $1.4 \pm 0.1 M_{\odot}$  and  $0.82 \pm 0.08 M_{\odot}$ , respectively.

## KOI-1786.01

We observed four times with SOPHIE the star KOI-1786 which host a transiting candidate with a period of 24.7 days. We measured a large and eccentric ( $e \sim 0.32$ ) radial velocity variation in phase with *Kepler* ephemeris (see Table 16 and Fig. 1) that is due to an eclipsing binary. Assuming a host star of  $0.49 M_{\odot}$  (Ba12), we find a mass for the transiting companion of  $0.232 \pm 0.014 M_{\odot}$ . As for KOI-340.01, this planetary candidate is also listed in the *Kepler* eclipsing binary catalog.

## 4.4. Diluted binaries

We also find in our sample several eclipsing binaries for which the transit is diluted by another star in the system (hierarchical system) or in foreground/background (blend):

## KOI-51.01

KOI-51.01 is a candidate on a  $\sim 10.4$ -day orbit. The digitalized sky survey shows three close-in stars within a nebulousity at the coordinates of this candidate. We roughly estimated the magnitude of each component seen on the POSSII F-DSS2 image using aperture photometry. We find that the transit would have a depth in-between 14% and 21% depending on which star is transited. We thus conclude that this candidate is a diluted binary. We note that this planetary candidate is also classified as a detached eclipsing binary in the *Kepler* eclipsing binary catalog.

## KOI-190.01

KOI-190.01 is a  $\sim 12.3$  day-period candidate. We took two SOPHIE spectra at orbital phase 0.23 and 0.78 (see Table 4). The spectra revealed a double-line binary (see fig. 2). The main component of this double-line present a significant radial velocity variation in phase with the *Kepler* ephemeris and with a semi-

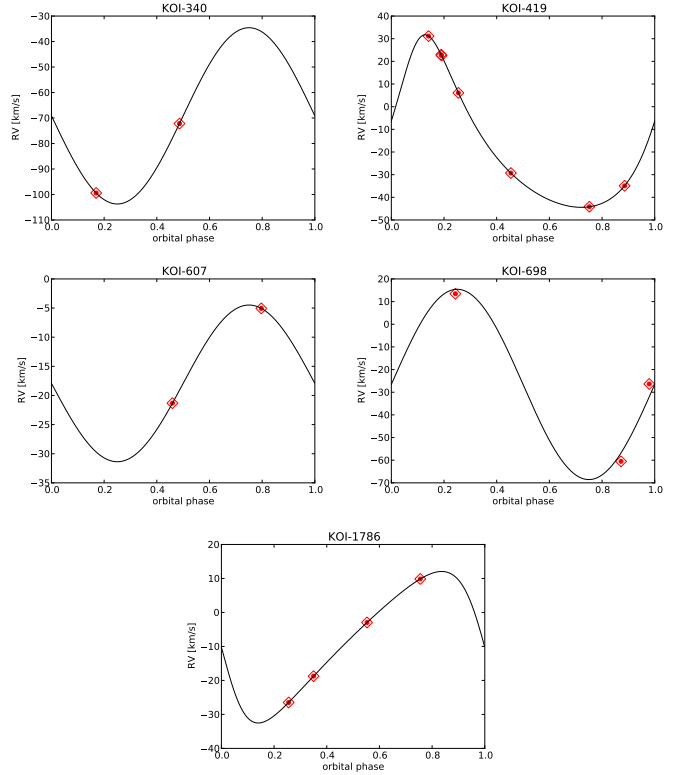


**Fig. 1.** Phase-folded radial velocity SOPHIE measurements of undiluted binaries where phase zero correspond to the transit epoch. The black line displays the best circular or eccentric model.

amplitude of  $K = 14.186 \pm 0.059 \text{ km s}^{-1}$  assuming a circular orbit. If this primary star has a mass of  $1 M_{\odot}$ , its companion would have a mass of about  $0.17 M_{\odot}$ . The second and fainter component also exhibits a radial velocity variation not in phase with the *Kepler* ephemeris and compatible with a drift of  $\sim 42 \text{ m.s}^{-1}.\text{d}^{-1}$ . As the fainter component is not varying in anti-phase with the primary star with a larger amplitude, this system is probably a triple system with a low-mass star eclipsing the main component of a long-period binary. This candidate is thus a diluted eclipsing binary, likely in a hierarchical triple system.

## KOI-418.01

We observed twice with SOPHIE KOI-418.01, a candidate on a 22.4 day-period orbit. The observed CCFs revealed the presence of a blending companion (see fig. 2). This blend scenario is confirmed by the bisector (see Table 9) which is clearly correlated with the radial velocities (Bouchy et al. 2009b). We conclude that this candidate is a diluted eclipsing binary.

## KOI-425.01

KOI-425.01 is a  $\sim 5.4$  days period candidate that was observed twice by SOPHIE. As for KOI-190.01, the CCFs show two peaks (see fig. 2) for which the main one is varying in phase with the *Kepler* ephemeris. Assuming a circular orbit, we find a semi-amplitude of  $K = 14.53 \pm 0.79 \text{ km s}^{-1}$ . Assuming a  $1 M_{\odot}$  stellar mass, the transiting companion would have a mass of  $\sim 0.13 M_{\odot}$ . The second and fainter peak presents no significant radial velocity variation. We thus conclude that KOI-425 is a diluted eclipsing binary, likely in a triple system.

## KOI-609.01

KOI-609.01 is candidate that transits its host-star every  $\sim 4.4$  days. We observed it twice with SOPHIE. The observations revealed a double-line spectroscopic binary (see fig. 2). We analyzed the radial velocity variation of both peaks in the CCF (see Table 13) and found that the primary peak presents no significant radial velocity variation. On the other hand, the secondary and fainter peak is varying in phase with the *Kepler* ephemeris with a semi-amplitude of  $K = 25.5 \pm 2.5 \text{ km s}^{-1}$  if the orbit is circular. Assuming a host-star mass of  $1M_{\odot}$ , the companion of this secondary star would have a mass of  $\sim 0.25 M_{\odot}$ . As the secondary peak is varying in phase with the *Kepler* ephemeris, we concluded that KOI-609 could be either a triple system or an unresolved background eclipsing binary.

## KOI-667.01

KOI-667.01 is a candidate on a  $\sim 4.3$ -day orbit. As for KOI-51, the digitalized sky survey shows a diffuse object at the coordinates of this candidate with at least three stars blended. We also perform rough aperture photometry of the few stars seen on the POSSII F-DSS2 image. We find that the undiluted transit depth should be in-between 6% and 12% depending on which star hosts the transit. We thus conclude that this candidate is not a planet but a diluted eclipsing binary.

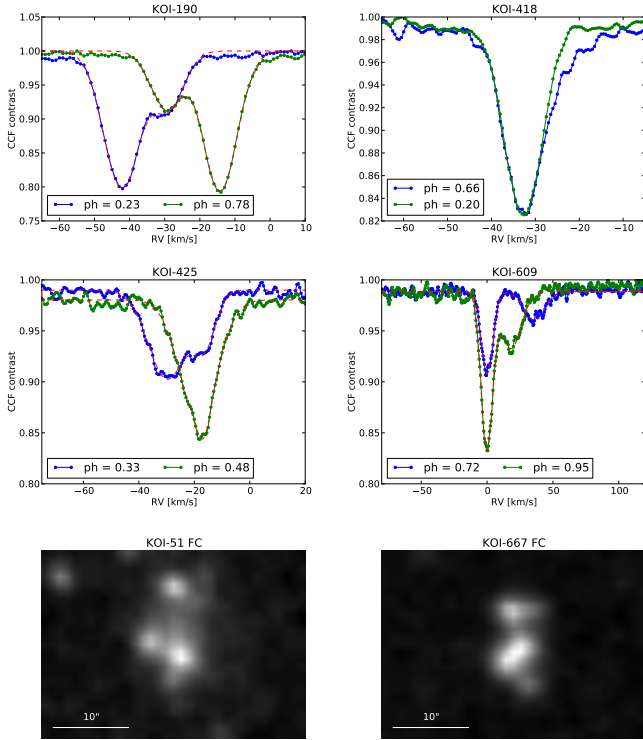


**Fig. 2.** CCFs of the diluted eclipsing binaries as function of radial velocities. Blue and green dot-lines display the observed CCFs and the dashed red lines are the multi-gaussian fit to the CCFs. The two lower panels are the SDSS finding charts (FC) of KOI-51.01 and KOI-667.01 that present several stars located within  $20'' \times 10''$ .

## 4.5. Unsolved cases

Some of the candidates present no significant radial velocity variations and are discussed below. Some of these candidates are members of the *Kepler* eclipsing binary catalog (Prša et al. 2011) with twice the orbital period which hints to a diluted equal-mass eclipsing binary. We believe that it is not a firm evidence of false positives since the planets KOI-135b (Bonomo et al. 2012) and KOI-206b (Hébrard et al., in prep.) are also in this list. We thus consider them as unsolved pending new follow-up observations.

## KOI-12.01

KOI-12.01 is a  $\sim 17.9$  day-period candidate orbiting a hot and fast rotating star with  $T_{\text{eff}} \sim 6400 \text{ K}$ . We took two SOPHIE measurements at phases 0.31 and 0.74 (see Table 2) and do not detect any significant radial velocity variation at the level of  $\sim 640 \text{ m s}^{-1}$  assuming a circular orbit (see Fig. 3). With about 18 days of period, the orbit may be eccentric. If it is the case, we may have missed the extremal phases. By fitting a rotational profile to the observed CCF, we find  $v \sin i_{\star} = 66 \pm 2 \text{ km s}^{-1}$ . Assuming a host star of  $1.17M_{\odot}$  (Ba12), we thus can put a  $3\text{-}\sigma$  upper limit on the mass of the companion of  $26.7M_{\text{Jup}}$ . With only two points with such large uncertainty, we can not constrain any blend scenario by analyzing the correlation between bisector and RVs. No mask effect is seen above  $1\text{-}\sigma$ . With a radius of about  $1.12R_{\text{Jup}}$ , the transiting companion is still compatible with a planetary or low-mass brown dwarf scenario or with a blend scenario.

## KOI-131.01

We observed twice KOI-131.01, a  $\sim 5.0$  day-period orbital-period candidate. The CCF revealed a fast rotating star with  $v \sin i_{\star} = 27 \pm 1 \text{ km s}^{-1}$ . We found no significant radial velocity variation at the level of  $\sim 800 \text{ m s}^{-1}$  (see Fig. 3). We can thus put an upper limit on the mass of the expected companion to be lower than  $14.3M_{\text{Jup}}$  assuming a circular orbit and a stellar mass of  $1.28M_{\odot}$  (Ba12). Our two measurements are not accurate enough to allow blend analysis using the bisector. No mask effect is seen above  $1\text{-}\sigma$ . The planetary and blend scenarios are still compatible with our data. We note that this candidate is also classified as an eclipsing binary (Prša et al. 2011) with twice the orbital period.

## KOI-192.01

KOI-192.01 is a  $\sim 10.3$ -day period candidate. We took two SOPHIE measurements at orbital phases 0.22 and 0.78 (see Table 5). The resulting radial velocities do not present any significant variation at a level of  $23 \text{ m s}^{-1}$  (see Fig. 3) assuming a circular orbit. If the orbit is slightly eccentric, we may not have observed KOI-192 at the extremal phases. From the CCF, we computed a  $v \sin i_{\star} = 11 \pm 1 \text{ km s}^{-1}$ . By analysis the spectra we obtained, we find a host star with  $T_{\text{eff}} = 5976 \pm 165 \text{ K}$ ,  $\log g = 4.46 \pm 0.15$  and  $[\text{Fe}/\text{H}] = -0.05 \pm 0.14$  dex in close agreement with the parameters published by Ba12. This correspond to a star with  $M_{\star} = 1.01^{+0.13}_{-0.11} M_{\odot}$  and  $R_{\star} = 1.03^{+0.12}_{-0.10} R_{\odot}$  with an age of  $3.5^{+6.3}_{-1.4} \text{ Gyr}$ .

We thus put a  $3\text{-}\sigma$  upper limit on the mass of the companion of  $0.59M_{\text{Jup}}$ . We cannot constrain any blend scenario within  $1\text{-}\sigma$  with our two bisector measurements. No significant mask effect

is seen up to the  $1-\sigma$  level. With a mass of less than  $0.59M_{\text{Jup}}$  and a radius of  $0.9 \pm 0.1R_{\text{Jup}}$ , the transiting companion is still compatible with a Saturn-like planet as well as with a blend. A high-contrast and high-resolution imaging would help to discard any potential background eclipsing binary within the exclusion radius of the centroid test (Batalha et al. 2010).

#### KOI-197.01

KOI-197.01 is a candidate in a  $\sim 17.3$ -day period orbit. We obtained twelve SOPHIE measurements (see Table 6). The resulting radial velocities do not present any significant variation at a level of  $12 \text{ m s}^{-1}$  (see Fig. 3). We computed a  $v \sin i_*$  of  $11 \pm 1 \text{ km s}^{-1}$ . Our spectral analysis revealed a host star with  $T_{\text{eff}} = 4995 \pm 126 \text{ K}$ ,  $\log g = 4.62 \pm 0.24$  and  $[\text{Fe}/\text{H}] = -0.11 \pm 0.06$  dex. This corresponds to an old star with  $M_* = 0.77 \pm 0.09 M_{\odot}$  and  $R_* = 0.74 \pm 0.08 R_{\odot}$ .

We thus put a  $3-\sigma$  upper limit on the mass of the companion of  $0.27M_{\text{Jup}}$ . No significant bisector variation is seen in the data, nor mask effect within  $1-\sigma$ . With a mass of less than  $0.27M_{\text{Jup}}$  and a radius of  $0.65 \pm 0.07 R_{\text{Jup}}$ , the transiting companion is still compatible with a Saturn-like planet or a blend. A high-contrast and high-resolution imaging would also help to discard any potential background eclipsing binary within the exclusion radius of the centroid test (Batalha et al. 2010).

#### KOI-201.01

KOI-201.01 is a candidate that transits its host star every  $\sim 4.2$  days. We observed twice this candidate with SOPHIE (see Table 7). The resulting radial velocities do not present any significant variation at a level of  $33 \text{ m s}^{-1}$ . We found a  $v \sin i_*$  of  $9 \pm 1 \text{ km s}^{-1}$ . We find a host star with  $T_{\text{eff}} = 5526 \pm 231 \text{ K}$ ,  $\log g = 4.56 \pm 0.33$  and  $[\text{Fe}/\text{H}] = 0.28 \pm 0.15$  dex. This correspond to a star with  $M_* = 1.09^{+0.13}_{-0.16} M_{\odot}$  and  $R_* = 1.05 \pm 0.12 R_{\odot}$ .

We thus put a  $3-\sigma$  upper limit on the mass of the companion of  $0.6M_{\text{Jup}}$  (see Fig. 3). From our two bisector measurements, we cannot constrain any blend. We do not find a mask effect above  $1-\sigma$  level. With a radius of  $0.8 R_{\text{Jup}}$  and a mass of less than  $0.6 M_{\text{Jup}}$ , neither the transiting planet scenario nor the blend scenario is discarded by our data. We note that this candidate is also in the *Kepler* eclipsing binary catalog (Prša et al. 2011) with twice the orbital period.

#### KOI-410.01

As presented in Bouchy et al. (2011), we observed twice with SOPHIE the candidate KOI-410.01 in 2010 and found no significant variation that exclude at  $3-\sigma$  a planetary mass greater than  $3.4M_{\text{Jup}}$ . Ba12 improved the parameters of this candidate compared to Borucki et al. (2011b) and found a radius ratio of  $0.36151 \pm 1.36849$  by fitting a grazing eclipse to these 'V'-shaped events. Since we excluded any undiluted eclipsing binaries that could mimic such a large radius ratio, we suspect that this candidate is a blend without firm evidence.

#### KOI-611.01

KOI-611.01 is a candidate that orbits its host star in  $\sim 3.3$  days. We took two SOPHIE spectra of this candidate that do not show any significant radial velocity variation at the level of

$\sim 100 \text{ m s}^{-1}$  (see Table 14 and Fig. 3). We found a  $v \sin i_*$  of  $17 \pm 1 \text{ km s}^{-1}$ . Assuming a host star mass of  $1.09 M_{\odot}$ , we can exclude all companion with a mass greater than  $1.5 M_{\text{Jup}}$  with a  $3-\sigma$  confidence. Our two bisector measurements do not constrain any blend scenario. No mask effect is found in the data within  $1-\sigma$ . With an expected radius of  $0.65 R_{\text{Jup}}$ , the planetary scenario is still compatible with our data.

#### Candidates not observed with SOPHIE

We do not consider the remaining 6 candidates (KOI-22.01, KOI-63.01<sup>4</sup>, KOI-94.01<sup>5</sup>, KOI-127.01, KOI-183.01 and KOI-214.01) for follow-up observations on SOPHIE since there were followed up on other radial velocity facilities by the *Kepler* follow-up team (Marcy, private comm.). We consider them as unsolved cases.

### 5. The False Positive Rate of *Kepler* close-in giant candidates

From the initial list of 46 KOIs selected, 20 planets have been discovered by various teams, 7 are clear undiluted eclipsing binaries or brown dwarfs, 6 are diluted eclipsing binaries and the remaining 13 ones are still unsolved. This leads to a rate of  $43.5\% \pm 6.5\%$  of planets,  $15.2\% \pm 4.1\%$  of undiluted binaries,  $13.0\% \pm 4.3\%$  of diluted binaries, and finally  $28.3\% \pm 6.5\%$  of unsolved cases. The uncertainties were computed using 100,000 iterations of a bootstrap resampling technique. Each resampling consists in randomly selecting 46 candidates from the actual list of 46 objects observed, allowing for repetitions (see Raghavan et al. 2010). The fractions of planets, false positives and unsolved cases are computed for each iteration. The resulting distributions are approximately normal for planets and unsolved cases, but not for the diluted and undiluted binaries, which are better fitted by a binomial distribution. The relatively low number of these false positives is not sufficient to reach the limit in which the binomial distribution resembles a gaussian. In all cases, the quoted uncertainties correspond to the  $68.3\%$  confidence region. We note that these uncertainties correspond to the statistical error only, and do not include any potential systematic source of error, such as potential misclassification of candidates.

The false positive rate (FPR) of *Kepler* giant candidates with orbital period shorter than 25 days and with transit depth deeper than  $0.4\%$  is thus in-between  $28.3\%$  and  $56.5\%$ , depending on the true nature of the unsolved candidates (see Fig. 4, left pie chart). We can assure that none of the unsolved case is an undiluted eclipsing binary for which we would have detected a significant radial velocity variation. In that case, we can assume that the true nature of the unsolved cases follows the same proportion of planets and blends than the observed one. This means that  $76.9\%$  of them are low-mass planets and  $23.1\%$  are diluted eclipsing binaries. We finally find that out of the 46 selected giant planet candidates  $65.2\% \pm 6.3\%$  are actual planets,  $15.2\% \pm 4.1\%$  are undiluted eclipsing binaries (including transiting brown dwarfs), and  $19.6\% \pm 6.5\%$  are blends. The *Kepler* FPP for short-period giant planets is thus  $34.8\% \pm 6.3\%$ . We expect that if we had included the 8

<sup>4</sup> KOI-63 was presented by Sanchis-Ojeda et al. at the First *Kepler* Science Conference as a very likely misaligned planet.

<sup>5</sup> KOI-94.01 is a member of a multiple (4) system candidate and thus is very likely planet.

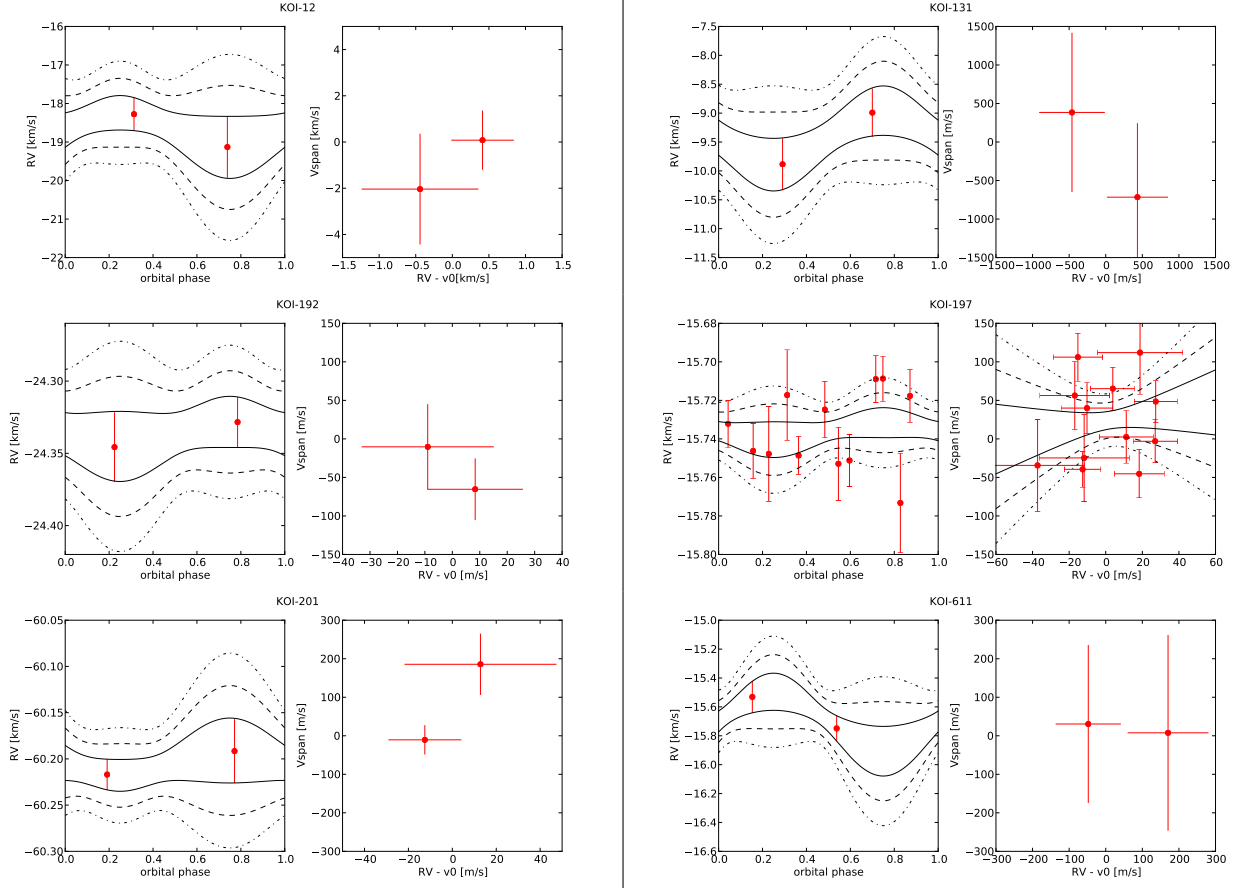


**Fig. 3.** Radial velocity (*left panels*) and bisector (*left panels*) SOPHIE measurements. Transits occur at phase zero. The straight line, dash-line and dash-dot lines represent the RV semi-amplitude and bisector variation limits at 1- $\sigma$ , 2- $\sigma$  and 3- $\sigma$ , respectively, assuming a circular orbit and a linear correlation between RV and bisector.

candidates with a vetting flag of 4, the FPP would be even higher.

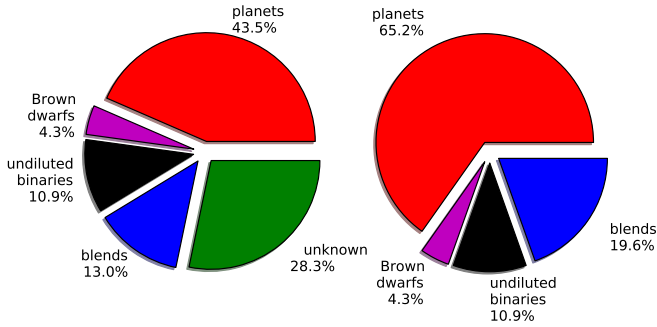


**Fig. 4.** Pie charts displaying the different ratio of each class of candidates. (*left*) Raw pie chart from the results of observations. (*right*) Pie chart assuming that the unsolved cases are either planets or blends with same proportions as observed.

## 6. Discussions

### 6.1. The Morton & Johnson estimation

The expected false positive fraction for the *Kepler* candidates has been estimated by M&J11 based on stellar population synthesis and galactic structure models. They also use the

results of a comprehensive survey of stellar multiplicity of solar-type stars within 25 pc of the Sun (Raghavan et al. 2010). Their main result is that the expected false positive ratio of *Kepler* candidates is below 10%. More precisely, they find that for about 90% of the candidates published by Borucki et al. (2011b), the probability that they are false positives is below 10%, and that about half have FPP below 5%. This result has motivated statistical analysis of planetary populations based on the *Kepler* candidates alone (Howard et al. 2011).

Our results seem to contradict the conclusions reached by M&J11. Indeed, our survey rejects a false positive rate smaller than 10% with 99.99% confidence level, considering the error on our FPP value. Moreover, when the FPPs of the individual candidates computed by M&J11 are considered (see Table 1), we find that the probability of having detected at least six false positives (our number of blended stellar systems, which are the only false positives considered in their analysis; see discussion below) is 0.4%. This probability was computed using 100,000 Monte Carlo simulations based on our sample of candidates. In each iteration, each candidate is randomly decided to be a planet or a false positive, depending on its expected FPP (see Table 1), and the resulting number of false positives ( $n_{FP}$ ) is recorded. The probability is obtained by integrating the distribution of  $n_{FP}$ .

There exists a number of reasons why the M&J11 analysis may lead to an underestimation of the *Kepler* FPP, at least for our sample of short-period giant planet candidates that



represents about 2% of all the *Kepler* candidates. Some of these are evoked by the authors in the final section of M&J11.

Chief among them is the fact that undiluted binaries are not considered as a source of false positives. M&J11 argue that this type of false positive can be effectively weeded out by a detailed analysis of the *Kepler* photometry alone. However, we have found that more than 10% of the followed-up candidates are actually low-mass-ratio binary stars, even excluding the two brown dwarfs reported here. This source of false positives is expected to be less important for smaller-radii candidates. However, as it is clearly shown by the cases of KOI-419 and KOI-698, stellar companions in eccentric orbits and with relatively long periods can produce single-eclipse light curves, even for greater mass ratios. It is difficult to imagine how these candidates can be rejected from photometry alone if grazing transits are to be kept.

However, even if we do not consider undiluted binaries, our survey has yielded at least six clear blended stellar systems, up to thirteen<sup>6</sup>. Our best estimate for the fraction of blended stellar systems is  $19.6\% \pm 6.5\%$ . We are therefore led to conclude that the estimation of M&J11 for this sample of candidates is underestimated. The first possible reason that comes to mind is an underestimation of the stellar density in the direction of the *Kepler* field. M&J11 use the TRILEGAL code of stellar population and Galactic structure (Girardi et al. 2005). The star count in TRILEGAL has been reported to show discrepancies smaller than 30 per-cent with a variety of stellar surveys for most of the sky, but it exhibits “major discrepancies” with fields at galactic latitude  $\lesssim 10$  degrees (Girardi et al. 2005). About 24% of the *Kepler* planetary candidate hosts would be affected by this effect. Although some of the simulated fields used to test TRILEGAL show a larger number of stars than observations (Girardi et al. 2005), we believe that a detailed analysis of the star count yield is warranted. This task is outside the scope of this paper.

A missing source of false positives in the M&J11 analysis are blended equal-mass eclipsing binaries, for which the difference in depth of the diluted primary and secondary eclipses will be too small to be detected by *Kepler* photometry. Since the mass ratio distribution of binary systems has a peak at  $q \sim 1$  and short-period ( $P < 100$  days; i.e. those with the highest probability of eclipsing) binary systems tend to have higher mass ratios (Raghavan et al. 2010), this type of eclipsing binaries might contribute significantly to the number of false positives. This source of false positives is expected to be more common for smaller planet candidates since odd/even depth difference is less significant.

Another possibility is an incorrect assumption for the planet radius distribution. M&J11 consider a continuous power law that increases towards small radii ( $dN/dR_p \propto R_p^{-2}$ ), but warn that if this is not so, false positives might be twice as numerous.

We also consider as a possible explanation an underestimation of the binary occurrence rate for massive blended stars. In their analysis, M&J11 assume that 75% of the stars with masses above  $1.5 M_\odot$  have binary companions. However, this is only a lower limit to the binary fraction of these stars (Raghavan

et al. 2010). On the other hand, TRILEGAL simulations like those used in M&J11 show that only between 0.02% and 0.4% – depending on galactic latitude – of blended stars will have masses above  $1.5 M_\odot$ . If the mass distribution of TRILEGAL is correct, then this underestimation will not have an important impact on the M&J11 FPP estimation.

Finally, a crucial factor in the number of blending systems affecting a given target is the area around it within which blends can reside. This area depends on the precision of the photocenter position, that *Kepler* measures for all of its candidates. M&J11 assumed a scaling law for the precision of the photocenter (their eq. 19) based on the host star magnitude and the depth of the observed transits. To be conservative, they assumed a minimum “radius of  $2''$  inside which a blend might reside”. If this blend exclusion radius is under-estimated, it will definitely under-estimate the proportion of potential background eclipsing binaries.

Even if this minimum exclusion radius of  $2''$ , i.e. equivalent to one pixel of *Kepler*, seems to be quite conservative, the number of transits observed for a given candidate should also be taken into account, since the position of the photocenter out of transit must be compared with the position in transit. Therefore, short-period candidates exhibiting a large number of transits should produce more precise measurements of the centroid shift. Since the scaling law is based on the measurements of a single very short period planet (Kepler-10 b,  $P = 0.84$  days), we believe that M&J11 might overestimate the ability of *Kepler* to identify blended stellar systems from astrometric measurements.

## 6.2. Comparison with other FPP estimations

Our value for the FPP is more in agreement with the one estimated by Borucki et al. (2011b) who estimated a FPP of  $< 20\%$  and  $< 40\%$  for KOIs with a vetting flag of 2 and 3, respectively. Gautier et al. (2010) discuss 21 good candidates with magnitude brighter than 14 followed up. They found 5 planets (24%), 8 rejected (38%) and 8 without conclusion. They then claimed a FPP in between 38% and 76% which is roughly compatible. Based on occultation depth found in the *Kepler* light-curves, Demory & Seager (2011) and Coughlin & López-Morales (2012) found a FPP of 14% and 11% respectively. This method shows its limitations since Demory & Seager (2011) did not reject four candidates that we found to be clear diluted binaries (KOI-190.01 and KOI-425.01) or undiluted eclipsing binaries (KOI-205.01 and KOI-698.01).

## 6.3. Extrapolation to longer orbital-period giant-planet candidates

Figure 5 displays the cumulative period distributions of planets (red line) and false positives (blue and black lines) for our candidates selection. The cumulative distribution of all candidates is shown as a dashed line. These distributions confirm the existence of a pile-up of giant planets at very short orbital period ( $\sim 3$  days). On the contrary, distributions of both diluted and undiluted binaries are relatively flat over the observed period range. We performed Kolmogorov – Smirnov tests on these distributions. We can reject the hypothesis that planets and undiluted binaries, or planets and blends have the same period distribution with a probability of more than 97.5%. We can also reject that planets and false positives have the same period

<sup>6</sup> This is, not considering the six unsolved cases for which we have not performed follow-up, and for which two are most likely planets.



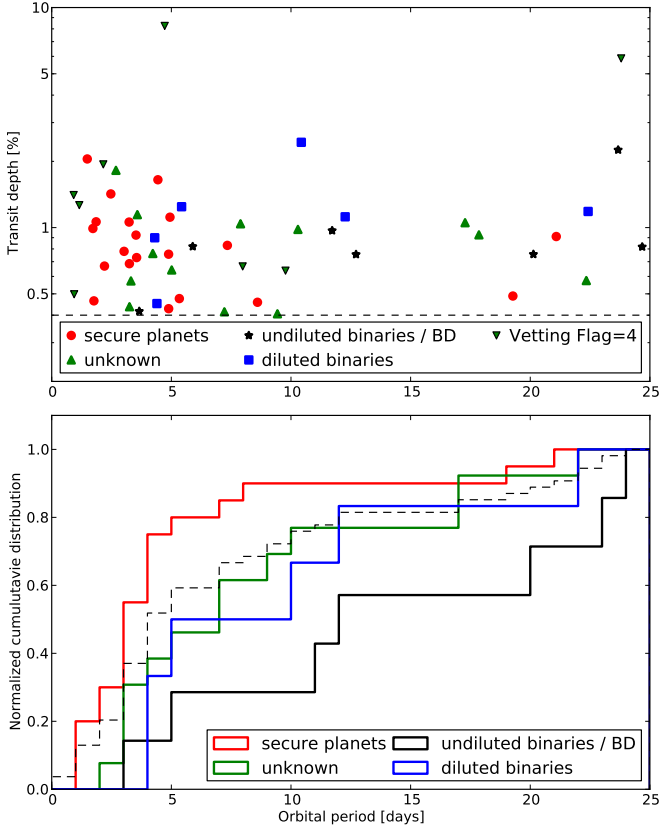


**Fig. 5.** (Top panel) Transit depth of the 46 selected KOIs as function of their orbital period. The different marks represent the different nature of the candidate. The dashed line represent the cut in transit depth applied to this selection. (Lower panel) Normalized cumulative distributions of the orbital period of the different class of candidates. The dashed black line displays the normalized cumulative distribution of the 46 selected candidates.

distribution with a probability of 99%. We thus find a different period distribution for planets and false positives. Indeed, no pile-up at very short period is expected for binaries which is the case for giant planets.

These results are compatible with the relative distribution of planet orbital periods and binary orbital periods (see Fig. 6). Indeed, we can express the FPP as follow :

$$\text{FPP}(P) = 1 - \frac{\pi_{pl}(P)}{\pi_{pl}(P) + \pi_{\star}(P)} \quad (2)$$

where  $\pi_{pl}(P)$  and  $\pi_{\star}(P)$  are the probabilities of having a planetary companion or a stellar companion (respectively) diluted or not for a given orbital period  $P$ .  $\pi_{\star}(P)$  is the sum of probabilities to have both a diluted or an undiluted binary :

$$\pi_{\star}(P) = \pi_{BB}(P) + \pi_{PT}(P) + \pi_{SB}(P) \quad (3)$$

where  $\pi_{BB}(P)$ ,  $\pi_{PT}(P)$  and  $\pi_{SB}(P)$  are the respective probabilities of having a background binary, a physical triple system or a spectroscopic binary. If we assume that all these binaries follow the same period distribution, we can thus reduce equation 3 to  $\pi_{\star}(P) \propto \pi_{SB}(P)$  and equation 2 to :

$$\text{FPP}(P) \propto 1 - \frac{1}{1 + \frac{\pi_{SB}(P)}{\pi_{pl}(P)}} \quad (4)$$

Figure 6 displays period distributions of both giant planetary companion detected by radial velocity (blue line) and stellar companion (red line). We take the [Raghavan et al. \(2010\)](#) result for the binary period-distribution:  $\log_{10}(P [\text{d}]) = \mathcal{N}(5.03, 2.28)$ , where  $\mathcal{N}(\mu, \sigma^2)$  is the normal distribution centered in  $\mu$  and with a standard deviation of  $\sigma$ . We note that this binary period distribution was calibrated only for binaries and triple systems of solar-type primary stars in the solar neighborhood. We may expect that distribution of binaries is different when dealing with non solar-type stars. The estimated FPP for *Kepler* giant planet candidates (fig. 6 dashed line) was computed using eq. 4 and calibrated in order to have  $\text{FPP} = 34.8\%$  when considering the same period range than our selected candidates period distribution.

We find that while the number of binaries increases with orbital period up to about 300 years, the number of detected giant planets decreases for periods in-between  $\sim 10$  days and  $\sim 200$  days. This so-called “period valley” detected by radial velocity surveys cannot be explained by an observational bias since it is easier to detect planets with short orbital period than planets with orbital period of a few years. This valley implies that the FPP is expected to increase in this range of periods, up to 40%. On the opposite, candidates with orbital period greater than  $\sim 200$  days are expected to have a FPP lower than 20%. We considered that the distribution of planets with orbital period greater than about three years is under-estimated due to observational bias and that the respective FPP should be lower.

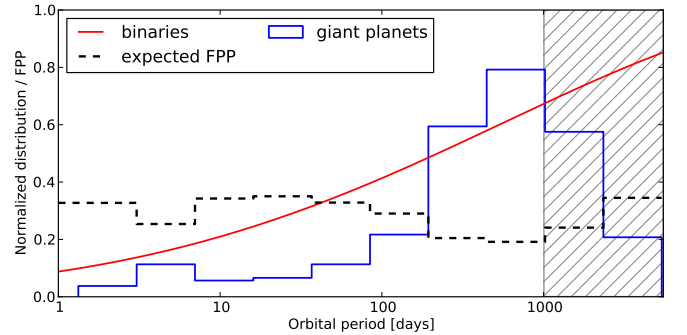


**Fig. 6.** Normalized distribution of 294 giant extrasolar planets discovered by the radial velocity technique to date with a mass greater than  $0.5 M_{\text{Jup}}$  (blue line). The normalized distribution of binaries within 3000 day-period from [Raghavan et al. \(2010\)](#) is displayed with the red line. The expected FPP distribution for giant *Kepler* candidates is over-plotted with the dashed black line. The hatched region represents planet orbital periods that we considered affected by observational bias. The FPP in this region is thus expected to be over estimated.

#### 6.4. Impact on exoplanet statistics

[Howard et al. \(2011\)](#) pointed out an under occurrence of hot jupiters at about 3 days seen by *Kepler* compared with Doppler surveys ([Howard et al. 2010](#); [Mayor et al. 2011](#)). This study assumed that impostors are negligible. As shown in Fig. 5, our sample, cleaned from impostors, presents a hot jupiter pile-up around 3-day periods. The under occurrence found by [Howard](#)

et al. (2011) might be explained by the 35% of false positives that dilute the hot jupiter pile-up found with Doppler surveys and confirmed by our cleaned sample.

Our measurement of the *Kepler* FPP, significantly larger than previous estimations for close-in giant planets, pointed out that impostors are not negligible in the *Kepler* list of candidates. If we assumed that the FPP of small candidates is also much larger than the one estimated by Morton & Johnson (2011), any exoplanet statistics considering *Kepler* candidates as planets will not be accurate.

The latter statement is not true for candidates in multiple for which the FPP is expected to decrease significantly as pointed out by Latham et al. (2011); Lissauer et al. (2012); Fabrycky et al. (2012).

### 6.5. Toward smaller candidates

A similar study on shallower transiting candidate with high-precision instruments such as HARPS-N on the 3.6-m TNG telescope or HiReS on the Keck-1 telescope is mandatory to constrain the true FPP value of *Kepler* small candidates. As an example, we estimated the HARPS-N radial velocity uncertainty for a 1-hour exposure as function of stellar magnitude based on our experiment with HARPS for the *CoRoT* follow-up (Santerne et al. 2011a) and assuming a non-rotating and non-active solar-type star and a systematic error of  $50 \text{ cm s}^{-1}$  at high S/N (Pepe et al. 2011). We selected all the *Kepler* candidates with an estimated planetary radius smaller than  $5 R_{\oplus}$ . We assumed for these small planet candidates a density of half the earth density, hence in between Neptune-like and Earth-like planets. We consider that the planet is detected in radial velocity if the amplitude (peak-to-peak) is greater than 3 times the RV uncertainty.

Out of the 1981 multi-transit candidates with a radius smaller than  $5 R_{\oplus}$ , we found that only 77 candidates, hence less than 4%, may be detected in radial velocity, including only 26 targets brighter than magnitude 12, and including only 16 candidates with radius smaller than  $3 R_{\oplus}$ .

## 7. Conclusion

From the overall list of 2321 *Kepler* candidates from Borucki et al. (2011b) and Ba12, we selected 46 of them that respect the criterion of having a transit depth greater than 0.4%, an orbital period of less than 25 days, a host star brighter than  $K_p = 14.7$  and a vetting flag different from four. We observed with the SOPHIE spectrograph at Observatoire de Haute-Provence 28 of them that were not previously announced as planets or followed up by other teams. We found nine new planets (Bouchy et al. 2011; Santerne et al. 2011c; Bonomo et al. 2012, Hébrard et al. in prep.) that increase the number of secured planets in this sample up to 20. We also found two interesting transiting brown dwarfs in the range  $25 - 80 M_{\text{Jup}}$  (Díaz et al. in prep.) that increase the number of objects in this range to five. We also found five undiluted eclipsing binaries and six clear diluted eclipsing binaries (triple hierarchical systems or background eclipsing binaries). We cannot conclude on a planetary nor false positive scenario for 13 of them due to photon noise limitations or lack of observations. More data with SOPHIE or with HiReS on Keck or with the new HARPS-N spectrograph mounted on the TNG-3.6m telescope would permit to conclude on these

objets. If we assume that these 13 candidates follow the same proportion of planets and blends than the observed one, we concluded that the false positive rate of *Kepler* giant planet on orbital period less than 25 days is  $34.8\% \pm 6.5\%$ . This value is clearly incompatible with the FPP  $\sim 5\%$  estimated by Morton & Johnson (2011) that did not take into account the probability of having an undiluted eclipsing binary in the *Kepler* data and under-estimate the probability of having a diluted binary.

Comparing the distribution of planets and binaries found by radial velocity surveys, we expect a FPP up to about 40% for giant planet candidates with orbital period in between  $\sim 10$  days and  $\sim 200$  days. Only the RV follow-up of a significant fraction of these long-period candidates can support this statement.

We note that if we remove the magnitude constraint as well as the vetting flag constraint from our selection criteria, this sample increases by 85 new candidates to a total number of 131 giant planet candidates. Following up these 85 candidates will strengthen our FPP value. This requires a larger telescope such as the TNG-3.6m telescope with HARPS-N or the Keck telescope with HiReS to follow these candidates up to magnitude  $K_p=16.2$ . This work indicates that only the RV follow-up of a significant amount of *Kepler* candidates will provide the real value of the FPP.

Only a small fraction of *Kepler* small candidates are suited for the radial velocity follow-up. These candidates should be followed in radial velocity to determine the true value of FPP and to fill the mass-radius diagram of Neptune and super-Earth like planets. This FPP value for small size candidates is required to correctly derive and discuss the distribution of transiting planet parameters.

In this paper, we also provide a list of clear diluted or undiluted binaries. Their analysis can contribute to improve the planet validation techniques (e.g. Fressin et al. 2011). *Spitzer* Space Telescope observation of these candidates should reveal a significant depth difference compared with *Kepler* (Desert et al. 2012).

**Acknowledgements.** We thank the technical team at the Observatoire de Haute-Provence for their support with the SOPHIE instrument and the 1.93-m telescope and in particular the essential work of the night assistants. We are grateful to the *Kepler* Team for giving public access to *Kepler* light curves and for publishing a list of interesting planetary candidates to follow-up. Financial support for the SOPHIE observations from the Programme National de Planétologie (PNP) of CNRS/INSU, France is gratefully acknowledged. We also acknowledge support from the French National Research Agency (ANR-08-JCJC-0102-01). R.F.D. is supported by CNES. NCS acknowledges the support by the European Research Council/European Community under the FP7 through Starting Grant agreement number 239953, as well as from Fundação para a Ciência e a Tecnologia (FCT) through program Ciência 2007 funded by FCT/MCTES (Portugal) and POPH/FSE (EC), and in the form of grants reference PTDC/CTE-AST/098528/2008 and PTDC/CTE-AST/098604/2008.

This research has made use of the Exoplanet Data Explorer at exoplanets.org and the NASA Exoplanet Archive, which is operated by the California Institute of Technology, under contract with the National Aeronautics and Space Administration under the Exoplanet Exploration Program. This publication makes use of data products from the Wide-field Infrared Survey Explorer and Two Micron All Sky Survey, which are joint projects of the University of California, Los Angeles, and the Jet Propulsion Laboratory/California Institute of Technology, and respectively the University of Massachusetts and the Infrared Processing and Analysis Center/California Institute of Technology, funded by the National Aeronautics and Space Administration and/or the National Science Foundation.

## References

Almenara, J. M., Deeg, H. J., Aigrain, S., et al. 2009, *A&A*, 506, 337

- Baglin, A., Auvergne, M., Boisnard, L., et al. 2006, 36th COSPAR Scientific Assembly, 36, 3749
- Bakos, G. A., Torres, G., Pál, A., et al. 2010, *ApJ*, 710, 1724
- Baranne, A., Queloz, D., Mayor, M., et al. 1996, *A&AS*, 119, 373
- Batalha, N. M., Rowe, J. F., Gilliland, R. L., et al. 2010, *ApJ*, 713, L103
- Batalha, N. M., Rowe, J. F., Bryson, S. T., et al. 2012, *arXiv:1202.5852*
- Boisse, I., Eggenberger, A., Santos, N. C., et al. 2010, *A&A*, 523, A88
- Bonomo, A. S., Santerne, A., Alonso, R., et al. 2010, *A&A*, 520, A65
- Bonomo, A. S., Hébrard, G., Santerne, A., et al. 2012, *A&A*, 538, A96
- Borucki, W. J., Koch, D. G., Basri, G., et al. 2010, *Science*, 327, 977
- Borucki, W. J., Koch, D. G., Basri, G., et al. 2011a, *ApJ*, 728, 117
- Borucki, W. J., Koch, D. G., Basri, G., et al. 2011b, *ApJ*, 736, 19
- Borucki, W. J., Koch, D. G., Batalha, N., et al. 2012, *ApJ*, 745, 120
- Bouchy, F., Isambert, J., Lovis, C., Boisse, I., Figueira, P., Hébrard, G., & Pepe, F. 2009a, *EAS Publications Series*, 37, 247
- Bouchy, F., Moutou, C., Queloz, D., & the *CoRoT* Exoplanet Science Team 2009b, *IAU Symposium*, 253, 129
- Bouchy, F., Hébrard, G., Udry, S., et al. 2009c, *A&A*, 505, 853
- Bouchy, F., Bonomo, A. S., Santerne, A., et al. 2011, *A&A*, 533, A83
- Brown, T. M. 2003, *ApJ*, 593, L125
- Brown, T. M., Latham, D. W., Everett, M. E., & Esquerdo, G. A. 2011, *AJ*, 142, 112
- Castelli, F., & Kurucz, R. L. 2004, *arXiv:astro-ph/0405087*
- Coughlin, J. L., & López-Morales, M. 2012, *AJ*, 143, 39
- Demory, B.-O., & Seager, S. 2011, *ApJS*, 197, 12
- Désert, J.-M., Charbonneau, D., Demory, B.-O., et al. 2011, *ApJS*, 197, 14
- Desert, J.-M., Charbonneau, D., Fressin, F., & Torres, G. 2012, *American Astronomical Society Meeting Abstracts*, 219, #414.02
- Dunham, E. W., Borucki, W. J., Koch, D. G., et al. 2010, *ApJ*, 713, L136
- Endl, M., MacQueen, P. J., Cochran, W. D., et al. 2011, *ApJS*, 197, 13
- Fabrycky, D. C., Lissauer, J. J., Ragozzine, D., et al. 2012, *arXiv:1202.6328*
- Fortney, J. J., Demory, B.-O., Désert, J.-M., et al. 2011, *ApJS*, 197, 9
- Fressin, F., Torres, G., Désert, J.-M., et al. 2011, *ApJS*, 197, 5
- Fressin, F., Torres, G., Rowe, J. F., et al. 2012, *Nature*, 482, 195
- Gautier, T. N., III, Batalha, N. M., Borucki, W. J., et al. 2010, *arXiv:1001.0352*
- Girardi, L., Groenewegen, M. A. T., Hatziminaoglou, E., & da Costa, L. 2005, *A&A*, 436, 895
- Girardi, L., Williams, B. F., Gilbert, K. M., et al. 2010, *ApJ*, 724, 1030
- Holman, M. J., Fabrycky, D. C., Ragozzine, D., et al. 2010, *Science*, 330, 51
- Howard, A. W., Marcy, G. W., Johnson, J. A., et al. 2010, *Science*, 330, 653
- Howard, A. W., Marcy, G. W., Bryson, S. T., et al. 2011, *arXiv:1103.2541*
- Jenkins, J. M., Borucki, W. J., Koch, D. G., et al. 2010, *ApJ*, 724, 1108
- Koch, D. G., Borucki, W. J., Rowe, J. F., et al. 2010, *ApJ*, 713, L131
- Kurucz, R. L. 1997, *The first ISO workshop on Analytical Spectroscopy*, 419, 193
- Latham, D. W., Borucki, W. J., Koch, D. G., et al. 2010, *ApJ*, 713, L140
- Latham, D. W., Rowe, J. F., Quinn, S. N., et al. 2011, *ApJ*, 732, L24
- Lissauer, J. J., Marcy, G. W., Rowe, J. F., et al. 2012, *ApJ*, 750, 112
- Marigo, P., Girardi, L., Bressan, A., et al. 2008, *A&A*, 482, 883
- Mayor, M., Marmier, M., Lovis, C., et al. 2011, *arXiv:1109.2497*
- Mayor, M., Marmier, M., Lovis, C., et al. 2011, *arXiv:1109.2497*
- Mazeh, T., Nachmani, G., Sokol, G., Faigler, S., & Zucker, S. 2011, *arXiv:1110.3512*
- Mislis, D., & Hodgkin, S. 2012, *arXiv:1202.1760*
- Morton, T. D., & Johnson, J. A. 2011, *ApJ*, 738, 170
- Moutou, C., Bruntt, H., Guillot, T., et al. 2008, *A&A*, 488, L47
- Muirhead, P. S., Johnson, J. A., Apps, K., et al. 2012, *ApJ*, 747, 144
- O'Donovan, F. T., Charbonneau, D., Mandushev, G., et al. 2006, *ApJ*, 651, L61
- Pál, A., Bakos, G. Á., Torres, G., et al. 2008, *ApJ*, 680, 1450
- Pepe, F., Mayor, M., Galland, F., et al. 2002, *A&A*, 388, 632
- Pepe, F., Lovis, C., Ségransan, D., et al. 2011, *A&A*, 534, A58
- Perruchot, S., Kohler, D., Bouchy, F., et al. 2008, *Proc. SPIE*, 7014
- Prša, A., Batalha, N., Slawson, R. W., et al. 2011, *AJ*, 141, 83
- Turck-Chièze, S., Palacios, A., Marques, J. P., & Nghiem, P. A. P. 2010, *ApJ*, 715, 1539
- Raghavan, D., McAlister, H. A., Henry, T. J., et al. 2010, *ApJS*, 190, 1
- Santerne, A., Endl, M., Hatzes, A., et al. 2011a, *Detection and Dynamics of Transiting Exoplanets*, St. Michel l'Observatoire, France, Edited by F. Bouchy; R. Díaz; C. Moutou; EPJ Web of Conferences, Volume 11, id.02001, 11, 2001
- Santerne, A., Díaz, R. F., Bouchy, F., et al. 2011b, *A&A*, 528, A63
- Santerne, A., Bonomo, A. S., Hébrard, G., et al. 2011c, *A&A*, 536, A70
- Santos, N. C., Israelian, G., & Mayor, M. 2004, *A&A*, 415, 1153
- Schneider, J., Dedieu, C., Le Sidaner, P., Savalle, R., & Zolotukhin, I. 2011, *A&A*, 532, A79
- Shporer, A., Jenkins, J. M., Rowe, J. F., et al. 2011, *AJ*, 142, 195
- Skrutskie, M. F., Cutri, R. M., Stiening, R., et al. 2006, *AJ*, 131, 1163
- Snedden, C. 1973, *ApJ*, 184, 839
- Sousa, S. G., Santos, N. C., Israelian, G., Mayor, M., & Monteiro, M. J. P. F. G. 2007, *A&A*, 469, 783
- Sousa, S. G., Santos, N. C., Mayor, M., et al. 2008, *A&A*, 487, 373
- Southworth, J. 2008, *MNRAS*, 386, 1644
- Szabó, G. M., Szabó, R., Benkő, J. M., et al. 2011, *ApJ*, 736, L4
- Tal-Or, L., Santerne, A., Mazeh, T., et al. 2011, *A&A*, 534, A67
- Torres, G., Fressin, F., Batalha, N. M., et al. 2011, *ApJ*, 727, 24



**Table 1.** List of the 46 selected candidates for follow-up with SOPHIE with  $K_p < 14.7$  & depth  $> 0.4$  % &  $P < 25$  d & Vetting flag  $\neq 4$ .

KIC	KOI	Period* [days]	$K_p^*$	Depth* [%]	FPP* [%]	Object nature <sup>†</sup>	Mass [ $M_{Jup}$ ]	Reference <sup>‡</sup>
11446443	1.01	2.47	11.3	1.42	1.0	planet / TrES-2	1.20	OD06
10666592	2.01	2.20	10.5	0.67	0.5	planet / HAT-P-7b	1.80	Pá08
10748390	3.01	4.89	9.1	0.42	6.0	planet / HAT-P-11b	0.08	Ba10
6922244	10.01	3.52	13.6	0.94	0.9	planet / Kepler-8b	0.60	Je10
5812701	12.01	17.86	11.4	0.93	4.5	no var	$< 26.7$	this work
9941662	13.01	1.764	10.0	0.46	0.5	planet / KOI-13b	$< 9.2$	Ma11, Sh11, Mi12
10874614	17.01	3.23	13.0	1.07	0.8	planet / Kepler-6b	0.67	Du10
8191672	18.01	3.55	13.4	0.72	1.0	planet / Kepler-5b	2.11	Ko10
11804465	20.01	4.44	13.4	1.67	1.1	planet / Kepler-12b	0.43	Fo11
9631995	22.01	7.89	13.4	1.06	2.8	unknown / no FUp	–	
6056992	51.01	10.43	13.8	2.58	2.7	blend	–	this work
11554435	63.01	9.43	11.6	0.41	3.2	unknown / No FUp	–	
6462863	94.01	22.34	12.2	0.57	4.8	unknown / no FUp	–	
5780885	97.01	4.89	12.9	0.74	0.9	planet / Kepler-7b	0.43	La10
8359498	127.01	3.58	13.9	1.16	0.9	unknown / no FUp	–	
11359879	128.01	4.94	13.8	1.12	1.1	planet / Kepler-15b	0.66	En11
7778437	131.01	5.01	13.8	0.69	1.3	no var	$< 14.3$	this work
9818381	135.01	3.02	14.0	0.79	0.8	planet / KOI-135b	3.23	Bon12
9651668	183.01	2.68	14.3	1.83	0.9	unknown / no FUp	–	
5771719	190.01	12.27	14.1	1.15	5.5	blend	–	this work
7950644	192.01	10.29	14.2	1.00	4.5	no var	$< 0.6$	this work
9410930	196.01	1.86	14.5	1.08	0.7	planet / KOI-196b	0.55	Sa11
2987027	197.01	17.28	14.0	1.08	4.6	no var	$< 0.32$	this work
6046540	200.01	7.34	14.4	0.85	2.4	planet / KOI-200b	0.44	Hé+
6849046	201.01	4.23	14.0	0.60	0.9	no var	$< 0.6$	this work
7877496	202.01	1.72	14.3	1.03	0.6	planet / KOI-202b	0.88	Hé+
10619192	203.01	1.49	14.1	2.09	0.7	planet / Kepler-17b	2.47	Dé11, Bon12
9305831	204.01	3.25	14.7	0.72	1.1	planet / KOI-204b	1.02	Bon12
7046804	205.01	11.72	14.5	1.00	5.3	BD	$\sim 35$	Dí+
5728139	206.01	5.33	14.5	0.50	1.3	planet / KOI-206b	2.9	Hé+
11046458	214.01	3.31	14.2	0.58	1.0	unknown / NoFUp	–	
10616571	340.01	23.67	13.1	2.12	100	SB1	560	this work
3323887	377.01	19.26	13.8	0.75	4.5	planet / Kepler-9b	0.25	Ho10
5449777	410.01	7.22	14.5	0.41	1.9	no var	$< 3.4$	Bou11
7975727	418.01	22.42	14.5	1.22	6.8	blend	–	this work
8219673	419.01	20.13	14.5	0.77	4.4	SB1	723	this work
9478990	423.01	21.09	14.3	0.91	5.9	planet / KOI-423b	18.00	Bou11
9967884	425.01	5.43	14.7	1.23	1.7	blend	–	this work
5443837	554.01	3.66	14.5	0.54	–	BD	$\sim 80$	Dí+
5441980	607.01	5.89	14.4	0.66	1.8	SB1	120	this work
5608566	609.01	4.40	14.5	0.43	1.3	blend	–	this work
6309763	611.01	3.25	14.0	0.43	1.1	no var	$< 1.5$	this work
6752502	667.01	4.31	13.8	1.01	10.2	blend	–	this work
7529266	680.01	8.60	13.6	0.44	3.0	planet / KOI-680b	0.62	Hé+
8891278	698.01	12.72	13.8	0.78	4.6	SB1	859	this work
3128793	1786.01	24.68	14.6	0.82	–	SB1	244	this work

\* Orbital period, Kepler magnitude ( $K_p$ ) and transit depth from Borucki et al. (2011b) and Ba12.

\* False Positive Probability as estimated by Morton &amp; Johnson (2011).

† no var: no significant RV variation; blend: triple system or background eclipsing binary; SB1: single-line spectroscopic binary; no FUp: no follow-up observation with SOPHIE; BD: Brown dwarf with mass in between  $25M_{Jup}$  and  $80M_{Jup}$ .

‡ Ba10: Bakos et al. (2010); Bon12: Bonomo et al. (2012); Bor11: Borucki et al. (2011b); Bou11: Bouchy et al. (2011); Dé11: Désert et al. (2011); Dí+: Díaz et al. (in prep.); Du10: Dunham et al. (2010); En11: Endl et al. (2011); Fo11: Fortney et al. (2011); Hé+: Hébrard et al. (in prep.); Ho10: Holman et al. (2010); Je10: Jenkins et al. (2010); Ko10: Koch et al. (2010); La10: Latham et al. (2010); Ma11: Mazeh et al. (2011); Mi12: Mislis &amp; Hodgkin (2012); OD06: O'Donovan et al. (2006); Pá08: Pál et al. (2008); Sa11: Santerne et al. (2011c); Sh11: Shporer et al. (2011).

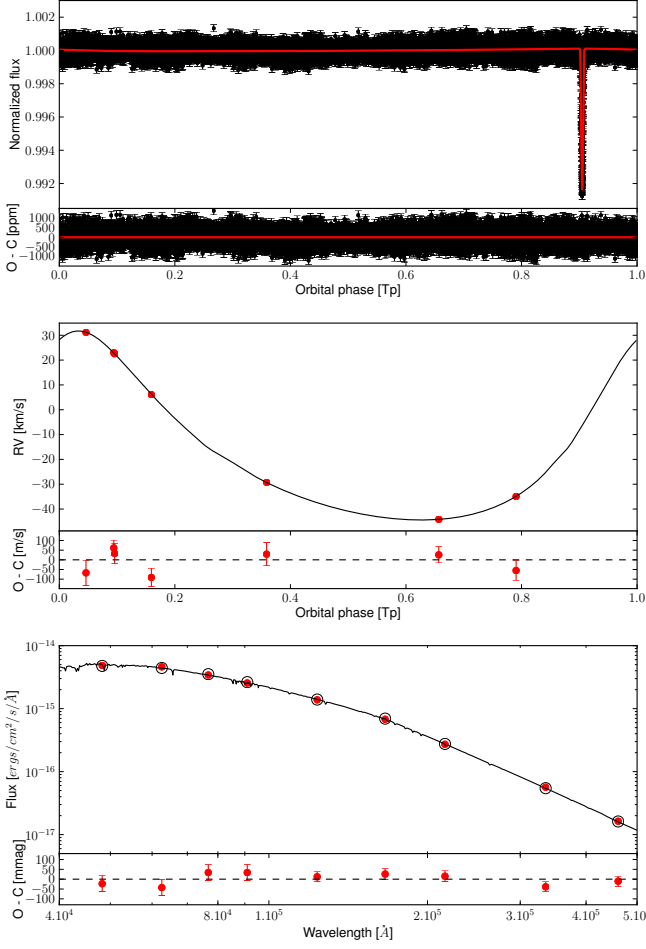


**Fig. 7.** KOI-419 light-curve (top panel), radial velocities (middle panel) and spectral energy distribution (bottom panel) with the best combined fit (red or black line). The phase zero correspond to the periastron epoch. The open circles in the bottom panel correspond to the best model integrated toward the same band-passes than the photometric measurements (red dots).

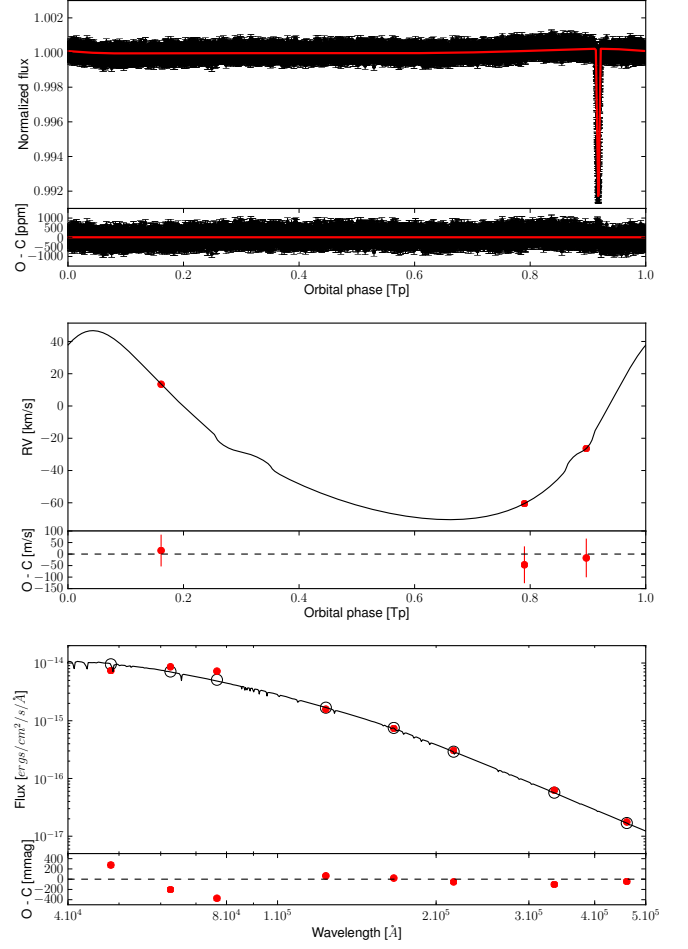


**Fig. 8.** KOI-698 light-curve (top panel), radial velocities (middle panel) and spectral energy distribution (bottom panel) with the best combined fit (red or black line). The phase zero correspond to the periastron epoch. The open circles in the bottom panel correspond to the best model integrated toward the same band-passes than the photometric measurements (red dots). The Rossiter-McLaughlin-like effect seen around phase 0.3 and 0.9 are due to the expected variation when the primary and secondary spectra are blended.

**Table 17.** Parameters for KOI-419

Primary and secondary stellar parameters	
Primary initial mass $M_{i,1}$ [ $M_{\odot}$ ]	$1.25 \pm 0.12^{\dagger}$
Secondary initial mass $M_{i,2}$ [ $M_{\odot}$ ]	$0.72 \pm 0.07^{\dagger}$
$\log(\text{age}[\text{yr}])$	$< 8$
Metallicity [Fe/H] [dex]	$-0.11 \pm 0.05^{\dagger}$
Binary parameters	
distance $d$ [pc]	$1153 \pm 17$
reddening $E(B - V)$	$0.20 \pm 0.03$
systemic radial velocity $v_0$ [ $\text{km s}^{-1}$ ]	$-17.88 \pm 0.03$
Orbital parameters	
Orbital period $P$ [d]	20.13151 (fixed)
Periastron epoch $T_p$ [BJD - 2400000]	$55910.088 \pm 0.008$
Inclination $i$ [°]	$87.211 \pm 0.016$
Eccentricity $e$	$0.334 \pm 0.001$
Argument of periastron $\omega$ [°]	$335.1 \pm 0.2$

<sup>†</sup> Assuming 10% uncertainty on the evolution tracks.

**Table 18.** Parameters for KOI-698

Primary and secondary stellar parameters	
Primary initial mass $M_{i,1}$ [ $M_{\odot}$ ]	$1.32 \pm 0.13^{\dagger}$
Secondary initial mass $M_{i,2}$ [ $M_{\odot}$ ]	$1.1 \pm 0.1^{\dagger}$
$\log(\text{age}[\text{yr}])$	$9.1 \pm 0.1^{\dagger}$
Metallicity [Fe/H] [dex]	$-0.4 \pm 0.04^{\dagger}$
Binary parameters	
distance $d$ [pc]	$1636 \pm 16$
reddening $E(B - V)$	$0.137 \pm 0.012$
systemic radial velocity $v_0$ [ $\text{km s}^{-1}$ ]	$-28.74 \pm 0.09$
Orbital parameters	
Orbital period $P$ [d]	12.71871 (fixed)
Periastron epoch $T_p$ [BJD - 2400000]	$55045.220 \pm 0.009$
Inclination $i$ [°]	$84.24 \pm 0.03$
Eccentricity $e$	$0.33 \pm 0.01$
Argument of periastron $\omega$ [°]	$328.7 \pm 0.3$

<sup>†</sup> Assuming 10% uncertainty on the evolution tracks.

**Table 2.** SOPHIE measurements of KOI-12.

BJD (-2 400 000)	RV [ $\text{km s}^{-1}$ ]	$\pm 1\sigma_{\text{rv}}$ [ $\text{km s}^{-1}$ ]	$V_{\text{span}}$ [ $\text{km s}^{-1}$ ]	$\pm 1\sigma_{V_{\text{span}}}$ [ $\text{km s}^{-1}$ ]	Texp [s]	S/N/pix @550nm
55617.71239	-19.132	0.799	-2.037	2.396	1006	23.1
55681.53719	-18.278	0.427	0.079	1.282	1312	43.1

**Table 3.** SOPHIE measurements of KOI-131.

BJD (-2 400 000)	RV [ $\text{km s}^{-1}$ ]	$\pm 1\sigma_{\text{rv}}$ [ $\text{km s}^{-1}$ ]	$V_{\text{span}}$ [ $\text{km s}^{-1}$ ]	$\pm 1\sigma_{V_{\text{span}}}$ [ $\text{km s}^{-1}$ ]	Texp [s]	S/N/pix @550nm
56010.59380	-9.886	0.449	0.384	1.034	1800	11.6
56012.64402	-8.991	0.417	-0.716	0.959	1504	10.1

**Table 4.** SOPHIE measurements of KOI-190.

BJD (-2 400 000)	$\text{RV}_A$ [ $\text{km s}^{-1}$ ]	$\pm 1\sigma_{\text{rv}_A}$ [ $\text{km s}^{-1}$ ]	$\text{RV}_B$ [ $\text{km s}^{-1}$ ]	$\pm 1\sigma_{\text{rv}_B}$ [ $\text{km s}^{-1}$ ]	Texp [s]	S/N/pix @550nm
55686.53761	-28.810	0.220	-42.267	0.101	3600	13.8
55705.50173	-29.612	0.161	-14.221	0.070	2525	19.0

**Table 5.** SOPHIE measurements of KOI-192.

BJD (-2 400 000)	RV [ $\text{km s}^{-1}$ ]	$\pm 1\sigma_{\text{rv}}$ [ $\text{km s}^{-1}$ ]	$V_{\text{span}}$ [ $\text{km s}^{-1}$ ]	$\pm 1\sigma_{V_{\text{span}}}$ [ $\text{km s}^{-1}$ ]	Texp [s]	S/N/pix @550nm
55754.44878	-24.346	0.024	-0.010	0.055	2274	17.3
55770.50760	-24.328	0.017	-0.065	0.040	3304	17.4

**Table 6.** SOPHIE measurements of KOI-197.

BJD (-2 400 000)	RV [ $\text{km s}^{-1}$ ]	$\pm 1\sigma_{\text{rv}}$ [ $\text{km s}^{-1}$ ]	$V_{\text{span}}$ [ $\text{km s}^{-1}$ ]	$\pm 1\sigma_{V_{\text{span}}}$ [ $\text{km s}^{-1}$ ]	Texp [s]	S/N/pix @550nm
55687.53172	-15.709	0.012	-0.003	0.028	3600	21.0
55765.49012	-15.748	0.025	-0.025	0.057	3600	15.2
55774.47483	-15.709	0.012	0.049	0.027	3600	21.2
55801.49572	-15.717	0.023	0.112	0.054	3600	15.5
55802.39087	-15.749	0.010	-0.040	0.023	3600	23.4
55804.45417	-15.725	0.015	0.003	0.034	3101	17.5
55806.39759	-15.751	0.013	0.106	0.031	3600	19.1
55810.40145	-15.773	0.026	-0.034	0.060	3600	12.7
55828.43357	-15.718	0.014	-0.045	0.031	3600	22.1
55831.39958	-15.732	0.012	0.065	0.028	3600	21.0
55833.37105	-15.746	0.014	0.040	0.033	3600	18.7
55857.35522	-15.753	0.019	0.056	0.044	3600	17.9

**Table 7.** SOPHIE measurements of KOI-201.

BJD (-2 400 000)	RV [ $\text{km s}^{-1}$ ]	$\pm 1\sigma_{\text{rv}}$ [ $\text{km s}^{-1}$ ]	$V_{\text{span}}$ [ $\text{km s}^{-1}$ ]	$\pm 1\sigma_{V_{\text{span}}}$ [ $\text{km s}^{-1}$ ]	Texp [s]	S/N/pix @550nm
55983.68634	-60.192	0.035	0.186	0.080	1800	9.4
55989.68601	-60.217	0.017	-0.011	0.038	1800	17.4

**Table 8.** SOPHIE measurements of KOI-340.

BJD (-2 400 000)	RV [ $\text{km s}^{-1}$ ]	$\pm 1\sigma_{\text{rv}}$ [ $\text{km s}^{-1}$ ]	$V_{\text{span}}$ [ $\text{km s}^{-1}$ ]	$\pm 1\sigma_{V_{\text{span}}}$ [ $\text{km s}^{-1}$ ]	Texp [s]	S/N/pix @550nm
55802.54571	-99.412	0.043	-0.089	0.098	600	10.3
55857.38486	-72.180	0.040	0.023	0.091	566	10.9



**Table 9.** SOPHIE measurements of KOI-418.

BJD (-2 400 000)	RV [ $\text{km s}^{-1}$ ]	$\pm 1\sigma_{\text{rv}}$ [ $\text{km s}^{-1}$ ]	$V_{\text{span}}$ [ $\text{km s}^{-1}$ ]	$\pm 1\sigma_{V_{\text{span}}}$ [ $\text{km s}^{-1}$ ]	Texp [s]	S/N/pix @550nm
55984.69997	-32.135	0.077	1.426	0.177	1800	7.8
55996.68516	-32.679	0.031	-0.035	0.071	2700	17.9

**Table 10.** SOPHIE measurements of KOI-419.

BJD (-2 400 000)	RV [ $\text{km s}^{-1}$ ]	$\pm 1\sigma_{\text{rv}}$ [ $\text{km s}^{-1}$ ]	$V_{\text{span}}$ [ $\text{km s}^{-1}$ ]	$\pm 1\sigma_{V_{\text{span}}}$ [ $\text{km s}^{-1}$ ]	Texp [s]	S/N/pix @550nm
55802.52069	-44.153	0.042	-0.045	0.096	900	10.3
55811.35898	22.576	0.053	-0.023	0.121	900	5.4
55831.46019	22.966	0.041	0.042	0.095	900	8.0
55973.69055	6.089	0.048	0.430	0.110	1703	4.0
55977.70619	-29.293	0.060	-0.067	0.138	900	7.1
56011.67515	31.153	0.066	0.034	0.152	900	8.0
56026.66141	-34.940	0.050	-0.235	0.115	900	5.1

**Table 11.** SOPHIE measurements of KOI-425.

BJD (-2 400 000)	$\text{RV}_A$ [ $\text{km s}^{-1}$ ]	$\pm 1\sigma_{\text{rv}_A}$ [ $\text{km s}^{-1}$ ]	$\text{RV}_B$ [ $\text{km s}^{-1}$ ]	$\pm 1\sigma_{\text{rv}_B}$ [ $\text{km s}^{-1}$ ]	Texp [s]	S/N/pix @550nm
55802.53448	-16.231	0.597	-29.718	0.442	900	8.4
55830.49421	-16.402	1.061	-18.546	0.410	900	6.9

**Table 12.** SOPHIE measurements of KOI-607.

BJD (-2 400 000)	RV [ $\text{km s}^{-1}$ ]	$\pm 1\sigma_{\text{rv}}$ [ $\text{km s}^{-1}$ ]	$V_{\text{span}}$ [ $\text{km s}^{-1}$ ]	$\pm 1\sigma_{V_{\text{span}}}$ [ $\text{km s}^{-1}$ ]	Texp [s]	S/N/pix @550nm
55828.46352	-21.323	0.029	0.073	0.067	900	13.3
55830.45215	-5.058	0.067	-0.121	0.153	900	7.5

**Table 13.** SOPHIE measurements of KOI-609.

BJD (-2 400 000)	$\text{RV}_A$ [ $\text{km s}^{-1}$ ]	$\pm 1\sigma_{\text{rv}_A}$ [ $\text{km s}^{-1}$ ]	$\text{RV}_B$ [ $\text{km s}^{-1}$ ]	$\pm 1\sigma_{\text{rv}_B}$ [ $\text{km s}^{-1}$ ]	Texp [s]	S/N/pix @550nm
55830.43654	0.074	0.413	35.830	1.590	900	7.9
55831.44062	-0.225	0.206	18.097	0.746	900	8.3

**Table 14.** SOPHIE measurements of KOI-611.

BJD (-2 400 000)	RV [ $\text{km s}^{-1}$ ]	$\pm 1\sigma_{\text{rv}}$ [ $\text{km s}^{-1}$ ]	$V_{\text{span}}$ [ $\text{km s}^{-1}$ ]	$\pm 1\sigma_{V_{\text{span}}}$ [ $\text{km s}^{-1}$ ]	Texp [s]	S/N/pix @550nm
55828.47808	-15.749	0.089	0.031	0.205	900	10.1
55830.48073	-15.531	0.111	0.008	0.254	900	8.9

**Table 15.** SOPHIE measurements of KOI-698.

BJD (-2 400 000)	RV [ $\text{km s}^{-1}$ ]	$\pm 1\sigma_{\text{rv}}$ [ $\text{km s}^{-1}$ ]	$V_{\text{span}}$ [ $\text{km s}^{-1}$ ]	$\pm 1\sigma_{V_{\text{span}}}$ [ $\text{km s}^{-1}$ ]	Texp [s]	S/N/pix @550nm
55832.44715	-26.362	0.084	0.777	0.192	600	6.2
55975.71173	13.455	0.069	-0.291	0.159	600	7.3
55983.70988	-60.514	0.080	0.703	0.183	1202	4.2

**Table 16.** SOPHIE measurements of KOI-1786.

BJD (-2 400 000)	RV [ $\text{km s}^{-1}$ ]	$\pm 1\sigma_{\text{rv}}$ [ $\text{km s}^{-1}$ ]	$V_{\text{span}}$ [ $\text{km s}^{-1}$ ]	$\pm 1\sigma_{V_{\text{span}}}$ [ $\text{km s}^{-1}$ ]	Texp [s]	S/N/pix @550nm
56013.58505	-26.488	0.060	0.655	0.138	1226	8.3
56040.59942	-18.745	0.177	-0.595	0.407	3600	13.3
56045.60870	-2.950	0.081	-0.025	0.185	1289	9.8
56050.59722	9.850	0.020	0.016	0.046	3600	12.1